

Time-series deformation monitoring over mining regions with SAR intensity-based offset measurements

CHAOYING ZHAO^{†‡}, ZHONG LU^{*§} and QIN ZHANG^{†‡}

[†]College of Geology Engineering and Geomatics, Chang'an University Xian, Xian, China

[‡]Key Laboratory of Western China's Mineral Resources and Geological Engineering,
Ministry of Education, Xian, China

[§]Cascades Volcano Observatory, U.S. Geological Survey, Vancouver, WA, USA

(Received 5 August 2012; in final form 27 October 2012)

Underground mining can induce large vertical displacements that often lead to the loss of coherence in repeat-pass interferometric synthetic aperture radar (SAR) images. Using SAR intensity images, this paper employs the image offset tracking method to map SAR slant range changes due to ground deformation over areas of mining. The rationale of slant range offset measurement with respect to the vertical deformation is analysed and the prerequisite of applying the slant range offset method to monitor vertical deformation is discussed. Results from the slant range offset method are used to produce time-series of cumulative ground displacements via least square estimate. We use six Advanced Land Observation Satellite (ALOS)-Phased Array L-band SAR (PALSAR) images over two coalfields in Inner Mongolia, China, to illustrate the proposed method and its effectiveness. We achieve deformation measurements with a precision of ~ 0.2 m, with the maximum vertical displacement over the mining sites reaching ~ 4.5 m. Finally, we use time-series results to outline common features identified in mining-induced deformation. Our results are supported by *in situ* investigations.

1. Introduction

Interferometric synthetic aperture radar (InSAR) uses phase measurements from two or more SAR images to derive measurements of surface deformation over large areas with an accuracy of centimetres to sub-centimetres (Massonnet and Feigl 1998, Hanssen 2001). InSAR has been used to map surface deformation due to various geophysical and man-made processes including mining activity (Massonnet and Feigl 1998). In order to maintain coherence in InSAR imagery, the deformation gradient should not be too large and time separation between SAR image acquisitions should not be too long (Massonnet and Feigl 1998, Sandwell and Price 1998).

Several studies have used InSAR to monitor ground deformation due to underground mining activity (Perski and Jura 1999, Carnec and Delacourt 2000, Yang *et al.* 2010). Multi-temporal InSAR methods, such as small baseline subset (SBAS) and persistent scatterer (PS) InSAR, have been employed to produce time-series of deformation measurements over mining regions (Jung *et al.* 2007, Ng *et al.* 2010). All of these studies use InSAR phase measurements to map surface deformation and require

*Corresponding author. Email: lu@usgs.gov

SAR images to be separated by short time intervals to maintain coherence. In most cases, mining-induced displacements are mostly vertical, spatially discontinuous and temporally non-linear. Such large surface displacements render the loss of InSAR coherence, resulting in the loss of information in areas of high deformation gradients (Massonnet and Feigl 1998, Hanssen 2001, Baran *et al.* 2005). Even for coherent areas, the interferometric fringes are often too saturated and aliased to be recovered with a phase unwrapping algorithm (Chen and Zebker 2001). Consequently, it is challenging to accurately monitor surface deformation in the regions of mining.

In this paper, we have applied the pixel offset tracking method to map large-gradient surface displacements due to mining activity. The method has been used to measure large deformation gradients due to glacial and co-seismic fault movements that would otherwise cause incoherence with traditional interferometry (Scambos *et al.* 1992, Michel *et al.* 1999, Strozzi *et al.* 2002, Leprince *et al.* 2007, Giles *et al.* 2009). At present, the method has not been used to monitor localized and mainly vertical deformation phenomena, such as mining-induced deformation. The offset measurements used in this method are based on fine and dense co-registration of two SAR images and can be used to measure slant range displacement to sub-pixel accuracy.

2. Method

Pixel offsets represent the change in the position of SAR backscattering features between different SAR images, which can be obtained through cross-correlation of SAR images using a moving window. At each pixel location, the cross-correlation is performed using a window size varying from 8 to 128 pixels (Zhang *et al.* 2011). During each co-registration, an oversampling factor of 2 is applied to increase the accuracy of the offset measurement. At each location, the offset estimate with the highest signal-to-noise ratio (SNR) is chosen as the pixel offset value. The global transformation between the two SAR images resulting from the difference in imaging geometry can be expressed as two second-order polynomials. Once the coefficients of the polynomials for both range and azimuth directions are estimated, the offset resulted from the difference in imaging geometry is then removed from the offset measurements. The remaining offset estimates are due to ground surface deformation in the flight direction and the line of sight (LOS) direction. In traditional interferometry, phase measurements are not sensitive to deformation in the flight direction; however, using azimuth offsets, it can be detected (e.g. Jung *et al.* 2009). Deformation in the LOS direction can be sensed by both traditional interferometry and the slant range offset from two SAR intensity images. As mining-induced surface deformation is nearly vertical, only the slant range offsets are used to monitor the mining deformation as the azimuth offset field is not sensitive to vertical motion.

As mentioned previously, mining activity may induce large deformation gradients, and if the deformation gradient is too large, or the time separation between SAR images is too long, InSAR phase measurements suffer from coherence loss. In this case, the slant range offset based on SAR intensity images is the only option for mapping the localized deformation. The geometry of slant range offset measurements with respect to the vertical deformation is shown in figure 1.

Mining-induced surface displacement is mostly vertical and is purely vertical at the centre of a subsidence cone (Yu and Zhang 2004). Assuming the horizontal deformation can be neglected, the vertical deformation, Δh , that occurs between two SAR images can be calculated from the slant range difference, Δr , as follows:

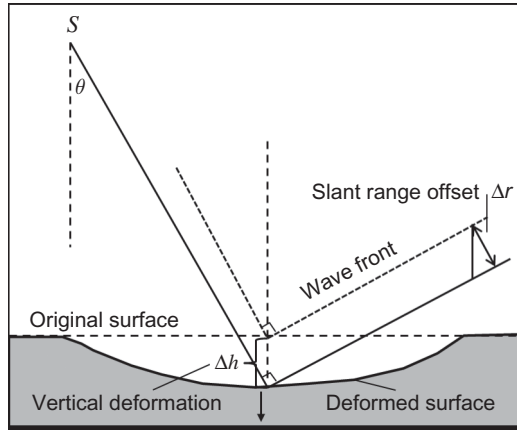


Figure 1. Geometry of slant range offset measurement with respect to the vertical deformation. S stands for the position of the satellite.

$$\Delta h = \frac{\Delta r}{\cos \theta}, \quad (1)$$

where θ is the incidence angle.

Previous studies of mapping large-gradient horizontal displacement have demonstrated that the precision of the pixel offset tracking method can reach 1/30 pixel (Fialko *et al.* 2001, Casu *et al.* 2011, Jung *et al.* 2011). So, in theory, if the vertical deformation is as large as tens of centimetres (sub-pixel posting of a SAR image), it can be measured by the slant range offset.

To remove unreliable measurements, we estimate the standard deviation of the slant range offset map using a 5 pixel \times 5 pixel window. We then use a threshold of 0.3 to remove outliers from the offset measurements. Instead of using a Gaussian filter (Yun *et al.* 2007), we interpolate the low-reliable regions of the offset map using an inpainting algorithm developed by John D'Errico, freely available as the Matlab function `inpaint_nans.m` from the Matlab Central file exchange (<http://www.mathworks.com/matlabcentral/fileexchange/4551-inpaintnans>). A final range offset map is created and the slant range offset is converted to vertical displacement using Equation (1).

An offset map can be created from two SAR images. If multi-temporal SAR images are available, a time-series surface deformation measurements can then be obtained using a least square estimate (Casu *et al.* 2011). Similar to the phase-based SBAS procedure (Berardino *et al.* 2002), the cumulative time-series results can be achieved by trivial integration of offset estimates between adjacent acquisitions.

Unlike phase-based measurements used in traditional interferometry, the perpendicular baseline is not the most limiting factor in making offset estimate. Instead, the temporal change of SAR backscatter intensity images is the main limitation. Because the offset estimate is based on the intensity cross-correlation algorithm, changes in the near-surface moisture, vegetation and other environmental factors that modify the SAR backscatter return will reduce the accuracy of the offset estimate. To overcome this for this study area, the SAR data were acquired mainly in the winter season when there is relatively less vegetation and precipitation.

3. Data and study area

We test our method of monitoring vertical surface displacement due to underground mining at two coalfields, Bulianta and Shangwan, located at the border between Inner Mongolia and Shaanxi provinces, China (figure 2(a)). Mining at this area has been undertaken since 2006. The full caving long-wall mining technique is used in these coalfields (unpublished report). The length of each long wall is around 6 km, which was segmented into 4–5 sections of similar length during the mining process. The width of each long wall is about 300 m. This layout is shown in figure 2(a). Located in the southeast corner of figure 2(a) is Daliuta coalfield, another long-wall mining site, where mining conditions are nearly identical to Bulianta and Shangwan coalfields. Ground-based levelling has been used to study subsidence at Daliuta (Wei *et al.* 1999).

A total of six ALOS-PALSAR images acquired in winter season between the end of 2006 and the beginning of 2011 are used in this study and in total 15 offset pairs are generated. The maximum perpendicular baseline is ~ 4.5 km and the maximum temporal baseline is ~ 4 years. The incidence angle is 38.7° in the central research region, so the slant range and ground range ratio is 1:1.6. In order to maintain a high spatial resolution, fine beam double-polarization (FBD) images are oversampled in the range direction to match the range posting of the fine beam single-polarization (FBS)

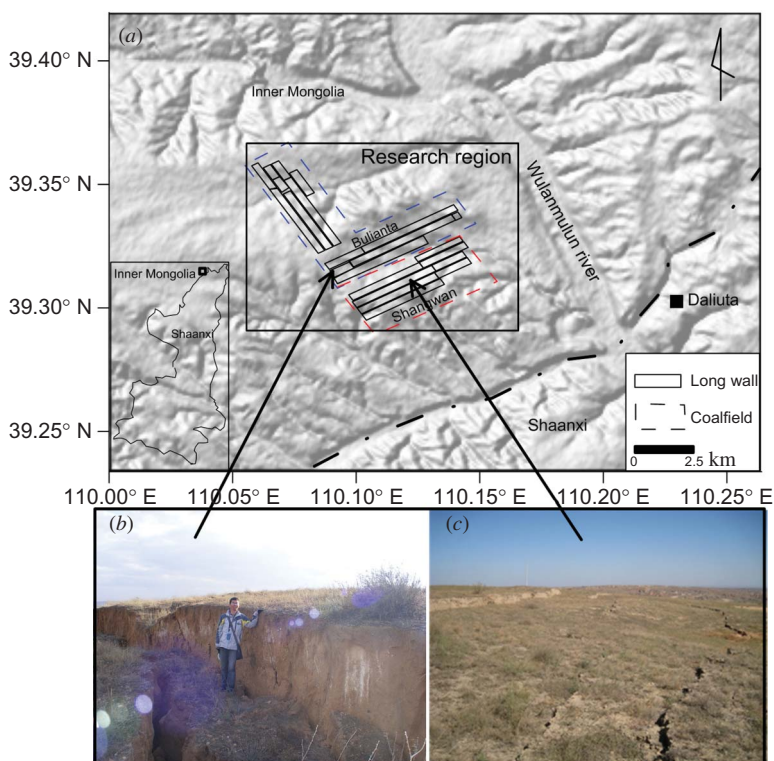


Figure 2. Research background map (a), two coalfields are outlined with red- and blue-dashed polygons, in which several long walls are shown with solid rectangles. The large rectangle represents the InSAR research region, which will be shown in figures 3 and 4. Photos are taken in November 2011 over Bulianta coalfield (b) and Shangwan coalfield (c).

mode (Sandwell *et al.* 2008), resulting in a slant range pixel posting of ~ 4.7 m and an azimuth pixel posting of ~ 3.1 m. Fine-scale offset measurements between images were calculated using the procedure described in section 2. Multiple independent offset measurements between different acquisitions were also used to increase the precision of time-series offset estimates.

4. Results and analysis

4.1. Comparison of InSAR phase measurement and image correlation offset results

At the mining sites in our study area, we find that the large ground deformation gradients induced by underground mining activity exceed the resolution of traditional interferometry phase measurements. This has resulted in the loss of coherence, even for the shortest time span (46 days) of L-band (wavelength of 23.6 cm) ALOS-PALSAR images. Figure 3(a) shows the unwrapped phase image generated from SAR images separated by 46 days between 22 December 2006 and 6 February 2007. Two sites of subsidence are clearly detected. However, the interferogram is incoherent over much of the mining site where the largest deformation gradient is expected (figure 3(a)); hence, we cannot recover the deformation over these areas using traditional interferometry. This problem becomes more severe if the two SAR images are acquired at a longer time interval. Figure 3(b) shows an interferogram produced from SAR images with a time interval of nearly 3 years. We see that the coherence is totally lost over most of the

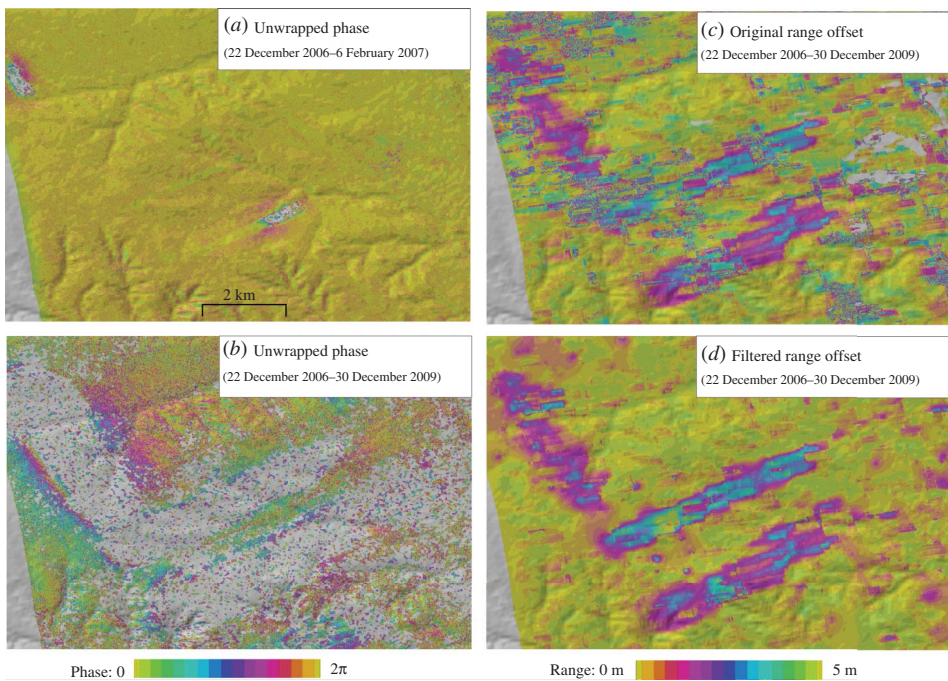


Figure 3. Illustration maps of mining-induced deformation over both Bulianta and Shangwan mining areas shown as research region in figure 2. (a) Unwrapped interferogram phase in 46 days, (b) unwrapped interferogram phase in ~ 3 years, (c) original slant range offset map in ~ 3 years and (d) filtered slant range offset map in ~ 3 years.

mining fields. However, using the pixel offset tracking method, the fine-scale range offset measurements can clearly map the vertical displacement based on this pair of SAR images (figure 3(c)). Figure 3(d) is a filtered slant range offset map produced using the procedure described in section 2, which effectively removes noise from the original range offset map (figure 3(c)). The extents of deformation are consistent with the long-wall mining plans (see figure 2 (a)). The maximum vertical deformation amounts to ~ 4.5 m, which is equivalent to about one slant range pixel posting.

4.2. Cumulative time-series mining subsidence maps

Based on a least square inversion using 15 slant range offset maps calculated from multi-temporal SAR images, cumulative slant range offset time-series maps can be produced on a pixel-by-pixel basis (figure 4). In each frame of figure 4, the mining

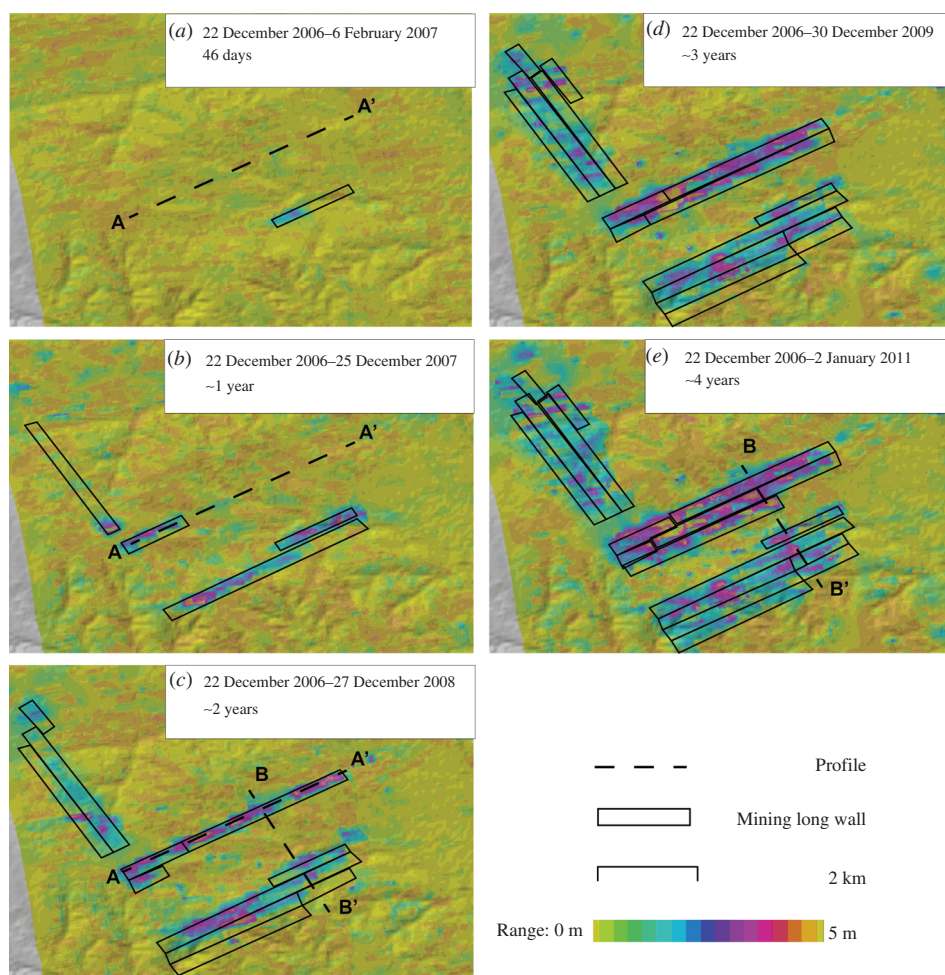


Figure 4. Cumulative slant range offset time-series maps over both Bulianta and Shangwan mining areas shown as research region in figure 2. Solid rectangles in each frame indicate mining long wall in the corresponding time interval. Two dashed lines A-A' and B-B' indicate the locations of profiles in figure 5.

layout during the corresponding monitoring periods is superimposed. We see that the regions of deformation are highly consistent with the extent of underground mining activity. Even though InSAR phase coherence is lost in 46 days due to large-gradient displacement, range offset measurements can clearly track down the ground surface subsidence for ~ 4 years.

The results from cumulative deformation time-series over two profiles (A-A' and B-B' in figure 4) are shown in figure 5. The precision of the slant range offset can be estimated during the 1st time period along the profile A-A' because there was no mining activity during that period. The standard deviation is 0.2 m, which accounts for 1/25 of a slant range pixel. This precision is similar to those reported elsewhere (Fialko *et al.* 2001, Casu *et al.* 2011, Jung *et al.* 2011).

During the 2nd time period (about 1 year after the reference image of 22 December 2006), the length of the deformed area along profile A-A' is around 2 km, which is a little bit longer than the planned mining length during that period (figure 4(b)), suggesting deformation extends beyond the extent of the mine. The average deformation is 1.85 m in the slant range direction and the maximum deformation reaches 4 m in the centre of subsidence cone (figure 5(a)). We find that a Gaussian curve can fit the land subsidence pattern very well (figure 5(a)). The Gaussian distribution curve is one of the widely accepted mining subsidence curves and has been applied to predict mining subsidence by, e.g. Litwinsky (1956) and Yu and Zhang (2004).

During the 3rd period (about 2 years after the reference image), we see that the deformed area continued to expand (figure 4(c) and figure 5(a)), and then stopped growing, as no mining activity was conducted over profile A-A' after the 3rd period. We have found that a Gaussian curve can fit the subsidence at each segment (length

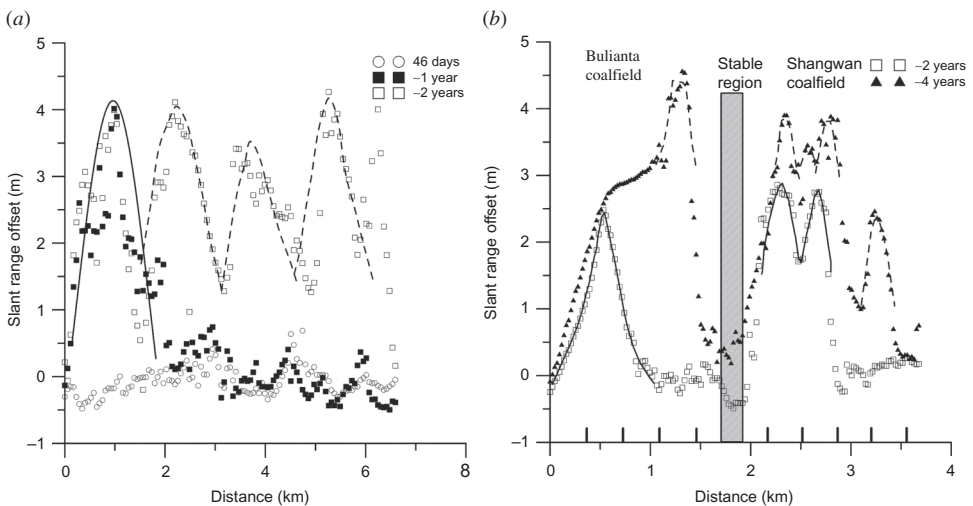


Figure 5. Cumulative time-series deformation results along two profiles indicated in figure 4: (a) profile A-A' along one of the long walls over the Bulianta coalfield, and (b) profile B-B' across seven long walls: Three from the Bulianta coalfield in the north and four from the Shangwan coalfield in the south. The bars near the bottom of figure 5(b) mark the boundaries of mining segments, each of which is about 300 m. The best-fit Gaussian distribution curves for the subsidence measurements along or across different mining segments are shown as solid or dashed lines.

of ~ 1.5 km). Each segment of the long-wall mines was supported by a safety pillar at each end, designed to stop the spread of subsidence. Overall, the average deformation is ~ 2.86 m and the maximum slant range deformation is up to 4 m over profile A-A'.

The regularity of the deformation pattern produced by mining across the long walls is demonstrated by observations from profile B-B'. Firstly, two coalfields can clearly be distinguished by a stable region between the two coalfields, which is indicated by a grey bar in figure 5(b) (i.e. no mining activity and no ground surface displacement). Secondly, seven further subsidence cones (three from Bulianta coalfield and four from Shangwan coalfield) can be outlined by truncated Gaussian curves. In figure 5(b), solid Gaussian distribution curves indicate the deformation during the 3rd period, while dashed curves are the deformation during the 5th period (about 4 years after the reference image). Thirdly, the extent of deformation over each long wall is slightly wider than the width of long wall (300 m), and the deformation over the first two long walls from the left side of figure 5(b) are merged. Finally, we see that the surface deformation will continue if the neighbouring long walls are subject to mining.

Our measurements of spatial patterns of mine subsidence are similar to levelling measurements over Daliuta coalfield (Wei *et al.* 1999). In our study area, the maximum deformation in the slant range direction is up to 4 m, which corresponds to ~ 4.5 m of vertical subsidence. Metre-scale surface deformation and step-like subsidence phenomena have also been verified by *in situ* investigation in November 2011 (figures 2(b) and (c)).

5. Conclusions

The slant range offset method can be applied to measure vertical deformation induced by underground mining activity where traditional interferometry fails due to the loss of coherence as a result of large displacement gradients. The precision of the slant range offset method is 0.2 m in this study, and the spatial resolution is around 250 m due to the limited size of the sliding window used in correlation calculations. This spatial resolution has an impact on the applicability of the offset method to mine deformation mapping. The subsidence can be reliably detected only if the deformation dimension is larger than the offset resolution.

Using time-series, we can track the temporal evolution of surface deformation in conjunction with the progression of underground mining activities. We use this method to successfully record mining-induced deformation over a 4-year time period. We also see that the temporal and spatial extents of subsidence and subsidence cones fit a Gaussian curve well.

Acknowledgements

The first author, Chaoying Zhao, would like to thank the China Scholarship Council for the funding of 1-year postdoctoral research carried out at Cascades Volcano Observatory, U.S. Geological Survey (USGS). ALOS-PALSAR data are copyrighted JAXA/METI. This research is funded by Natural Science Foundation of China (Nos 41072266, 41274005 and 41274004), the Ministry of Land Resources, China (Nos 1212011220186 and 1212011220142) and USGS Volcano Hazards Program. Special thanks go to Yinlin Liu and Renyi Zhu for their field investigation.

References

- BARAN, I., STEWART, M. and CLAESSENS, S., 2005, A new functional model for determining minimum and maximum detectable deformation gradient resolved by satellite radar interferometry. *IEEE Transactions on Geoscience and Remote Sensing*, **43**, pp. 675–682.
- BERARDINO, F., FORNARO, G., LANARI, R. and SANSOSTI, E., 2002, A new algorithm for surface deformation monitoring based on small baseline differential SAR interferometry. *IEEE Transaction on Geoscience and Remote Sensing*, **40** pp. 2375–2383.
- CARNEC, C. and DELACOURT, C., 2000, Three years of mining subsidence monitored by SAR interferometry, near Gardanne, France. *Journal of Applied Geophysics*, **43**, pp. 43–54.
- CASU, F., MANCONI, A., PEPE, A. and LANARI, R., 2011, Deformation time-series generation in areas characterized by large displacement dynamics: the SAR amplitude pixel-offset SBAS technique. *IEEE Transaction on Geoscience and Remote Sensing*, **49**, pp. 2752–2763.
- CHEN, C.W. and ZEBKER, H.A., 2001, Two-dimensional phase unwrapping with use of statistical models for cost functions in nonlinear optimization. *Journal of the Optical Society of America A-Optics Image Science and Vision*, **18**, pp. 338–351.
- FIALKO, Y., SIMONS, M. and AGNEW, D., 2001, The complete (3-D) surface displacement field in the epicentral area of the 1999 Mw 7.1 Hector Mine earthquake, California, from space geodetic observations. *Geophysics Research Letter*, **28**, pp. 3063–3066.
- GILES, A.B., MASSOM, R.A. and WARNER, R.C., 2009, A method for sub-pixel scale feature-tracking using Radarsat images applied to the Mertz Glacier Tongue, East Antarctica. *Remote Sensing of Environment*, **113**, pp. 1691–1699.
- HANSEN, R., 2001, *Radar Interferometry: Data Interpretation and Error Analysis*, pp. 40–41 (The Netherlands: Kluwer Academic Publishers).
- JUNG, H.C., KIM, S.W., JUNG, H.S., MIN, K.D. and WON, J.S., 2007, Satellite observation of coal mining subsidence by persistent scatterer analysis. *Engineering Geology*, **92**, pp. 1–13.
- JUNG, H.S., LU, Z., WON, J.S., POLAND, M.P. and MIKLIUS, A., 2011, Mapping three-dimensional surface deformation by combining multiple-aperture interferometry and conventional interferometry: application to the June 2007 eruption of Kilauea volcano, Hawaii. *IEEE Geoscience and Remote Sensing Letters*, **8**, pp. 34–38.
- JUNG, H.S., WON, J.S. and KIM, S.W., 2009, An improvement of the performance of multiple aperture SAR interferometry (MAI). *IEEE Transaction on Geoscience and Remote Sensing*, **47**, pp. 2859–2869.
- LEPRINCE, S., BARBOT, S., AYOUB, F. and AVOUAC, J.P., 2007, Automatic and precise orthorectification, co-registration and sub-pixel correlation of satellite images, application to ground deformation measurements. *IEEE Transaction on Geoscience and Remote Sensing*, **45**, pp. 1529–1558.
- LITWINSZY, J., 1956, Application of the equation of stochastic processes to mechanics of loose bodies. *Archium Mechaniki Stosowanej*, **8**, pp. 393–411.
- MASSONNET, D. and FEIGL, K.L., 1998, Radar interferometry and its application to changes in the Earth's surface. *Review of Geophysical*, **36**, pp. 441–500.
- MICHEL, R., AVOUAC, J.P. and TABOURY, J., 1999, Measuring ground displacements from SAR amplitude images: application to the Landers earthquake. *Geophysical Research Letter*, **26**, pp. 875–878.
- NG, A.H.M., GE, L., YAN, Y.G., LI, X.J., CHANG, H.C., ZHANG, K. and RIZOS, C., 2010, Mapping accumulated mine subsidence using small stack of SAR differential interferograms in the southern coalfield of New South Wales, Australia. *Engineering Geology*, **115**, pp. 1–15.
- PERSKI, Z. and JURA, D., 1999, ERS SAR interferometry for land subsidence detection in coal mining areas. *Earth Observation Quarterly*, **63**, pp. 25–29.
- SANDWELL, D., MYER, D., MELLORS, R., SHIMADA, M., BROOKS, B. and FOSTER, J., 2008, Accuracy and resolution of ALOS interferometry: vector deformation maps of the

- father's day intrusion at Kilauea. *IEEE Transactions on Geoscience and Remote Sensing*, **46**, pp. 3524–3534.
- SANDWELL, D.T. and PRICE, E.J., 1998, Phase gradient approach to stacking interferograms. *Geophysical Research*, **103**, pp. 30183–30204.
- SCAMBOS, T.A., DUTKIEWICZ, M.J., WILSON, J.C. and BINDSCHADLER, R.A., 1992, Application of image cross-correlation to the measurement of glacier velocity using satellite image data. *Remote Sensing of Environment*, **42**, pp. 177–186.
- STROZZI, T., LUCKMAN, A., MURRAY, T., WEGMÜLLER, U. and WERNER, C., 2002, Glacier motion estimation using SAR offset-tracking procedures. *IEEE Transactions on Geoscience and Remote Sensing*, **40**, pp. 2384–2391.
- WEI, B.L., FAN, L.M. and YANG, H.K., 1999, On the surface deformation of coal mining in shallow coal seam. *Coal Geology of China*, **11**, pp. 44–48. (in Chinese).
- YANG, C.S., ZHANG, Q., ZHAO, C.Y., Ji, L.Y. and ZHU, W., 2010, Monitoring mine collapse by D-InSAR. *Mining Science and Technology*, **20**, pp. 696–700.
- YU, X.Y. and ZHANG, E.Q., 2004, *Mining Damage* (Beijing: China Coal Industry Publishing House). (in Chinese).
- YUN, S.H., ZEBKER, H., SEGALL, P., HOOPER, A. and POLAND, M., 2007, Interferogram formation in the presence of complex and large deformation. *Geophysical Research Letter*, **34**, pp. L12305, doi:10.1029/2007GL029745.
- ZHANG, L., DING, X.L. and LU, Z., 2011, Ground settlement monitoring based on temporarily coherent points between two SAR acquisitions. *ISPRS Journal of Photogrammetry and Remote Sensing*, **66**, pp. 146–152.